

Supporting Information
for
 β -Cyclodextrin- and adamantyl-substituted poly(acrylate)
self-assembling aqueous networks designed for controlled
complexation and release of small molecules

Liang Yan¹, Duc-Truc Pham¹, Philip Clements¹, Stephen F. Lincoln*¹, Jie Wang², Xuhong Guo*², and Christopher J. Easton³

Address: ¹Department of Chemistry, University of Adelaide, Adelaide, SA 5005, Australia,

²State Key Laboratory of Chemical Engineering, East China University of Science and Technology, Shanghai 200237, China and ³Research School of Chemistry, Australian National University, Canberra, ACT 0200, Australia

Email: Stephen F. Lincoln* - stephen.lincoln@adelaide.edu.au; Xuhong Guo* - guoxuhong@ecust.edu.cn

* Corresponding author

Additional titrations, spectra and data

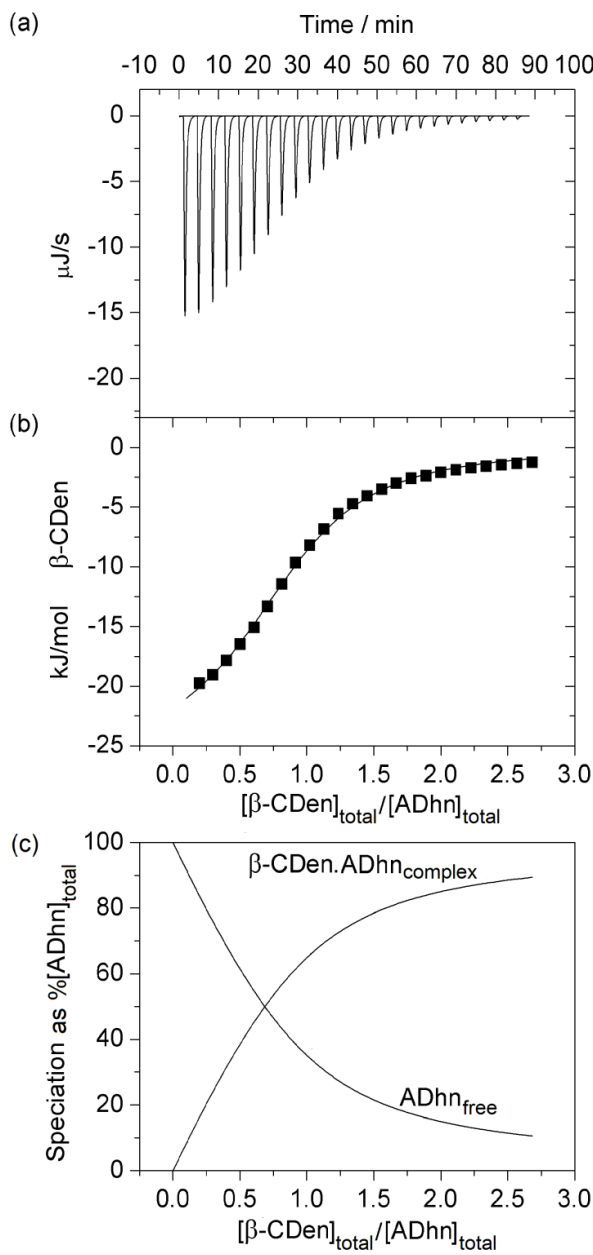


Figure S1: ITC data for the PAA β -CDen/PAAADhn system obtained in aqueous $\text{Na}_2\text{HPO}_4/\text{KH}_2\text{PO}_4$ pH 7.0 buffer at $I = 0.10 \text{ mol dm}^{-3}$. (a) Titration of 10 mm^3 aliquots of a 0.62 wt % PAA β -CDen ($[\beta\text{-CDen}] = 2.84 \times 10^{-3} \text{ mol dm}^{-3}$) into 1.46 cm^3 of 0.072 wt % PAAADen ($[\text{ADhn}] = 2.03 \times 10^{-4} \text{ mol dm}^{-3}$). (b) The solid curve shows the best fit of an algorithm for host-guest complexation between the β -CDen and ADhn substituents to the titration data. (c) Speciation plot showing the variation of $[\beta\text{-CDen-ADhn}]_{\text{complex}}$ and of $[\text{ADhn}]_{\text{free}}$ as a percentage of $[\text{ADhn}]_{\text{total}} = 100\%$.

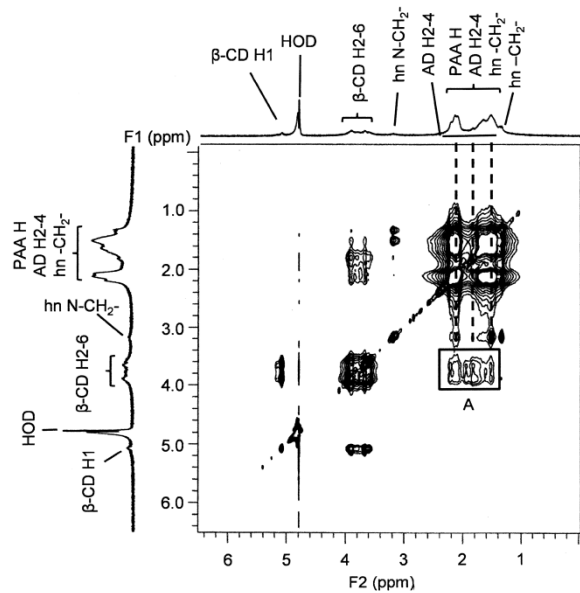


Figure S2: 2D NOESY ^1H NMR spectrum of 0.44 wt % PAA β -CDen ($[\beta\text{-CDen}] = 2.0 \times 10^{-3}$ mol dm^{-3}) and 0.67 wt % PAAADhn ($[\text{ADhn}] = 2.0 \times 10^{-3}$ mol dm^{-3}) in D_2O $\text{Na}_2\text{HPO}_4/\text{KH}_2\text{PO}_4$ buffer at $\text{pD} = 7.0$ and $I = 0.10$ mol dm^{-3} at 298.2 K. The cross-peaks in box A are attributed to dipolar interactions the annular H3,5,6 protons of the β -CD of the β -CDen substituents and the H2-4 protons of the ADhn substituents.

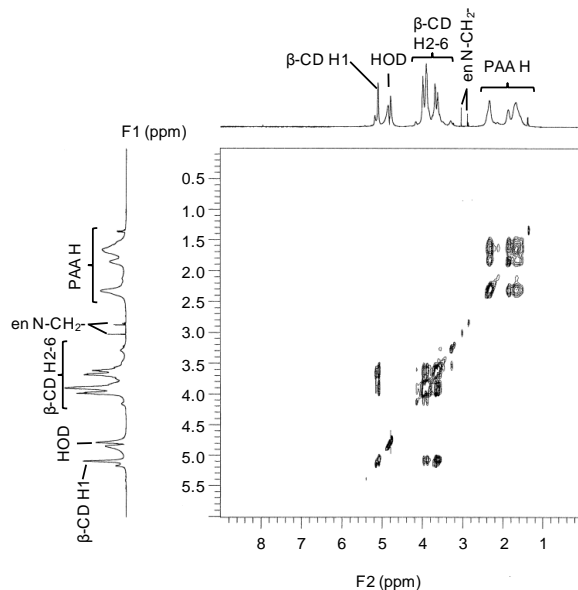


Figure S3: 2D NOESY ^1H NMR spectrum of 0.44 wt % PAA β -CDen ($[\beta\text{-CDen}] = 2.0 \times 10^{-3}$ mol dm^{-3}) in D_2O $\text{Na}_2\text{HPO}_4/\text{KH}_2\text{PO}_4$ buffer solution at $\text{pD} = 7.0$ and $I = 0.10$ mol dm^{-3} at 298.2 K.

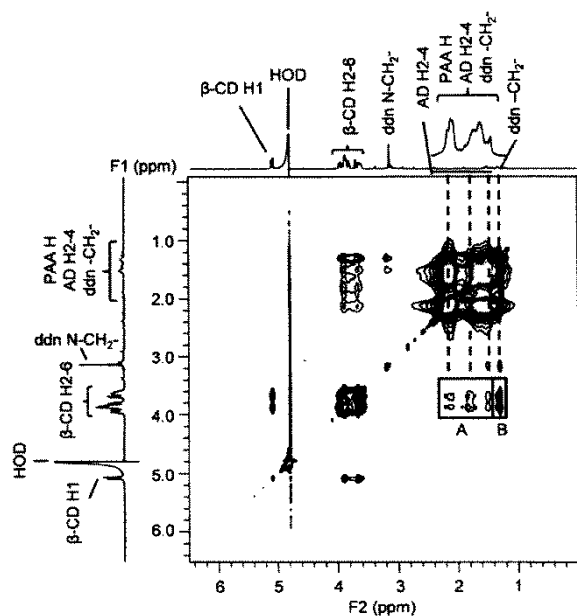


Figure S4: 2D NOESY ^1H NMR spectrum of 0.44 wt % PAA β -CDen ($[\beta\text{-CDen}] = 2.0 \times 10^{-3}$ mol dm^{-3}) and 0.70 wt % PAAADddn ($[\text{ADddn}] = 2.0 \times 10^{-3}$ mol dm^{-3}) in D_2O $\text{Na}_2\text{HPO}_4/\text{KH}_2\text{PO}_4$ buffer at $\text{pD} = 7.0$ and $I = 0.10$ mol dm^{-3} at 298.2 K. The cross-peaks in box A are attributed to dipolar interactions between the annular H3,5,6 protons of the β -CD of the β -CDen substituents and the H2-4 protons of the ADddn substituents. Cross-peaks in box B are attributed to dipolar interactions between the annular H3,5,6 protons of the β -CDen substituents and the tether dodecyl methylene protons (ddn- CH_2^-).

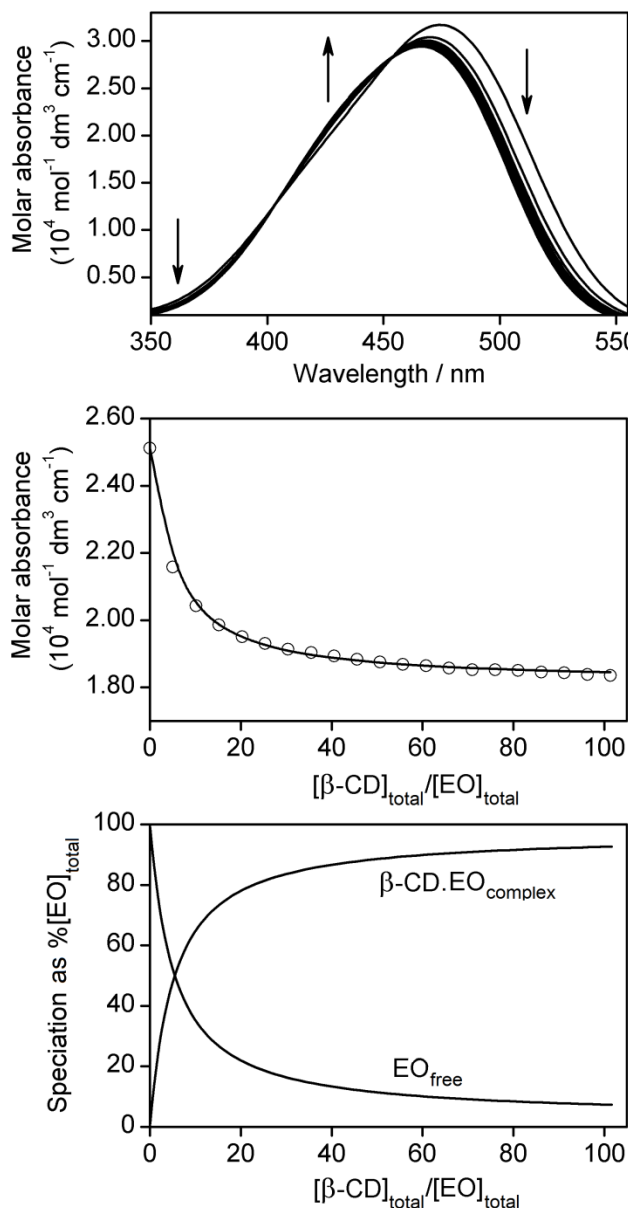


Figure S5: (Top) Molar absorbance variation of 1.5 cm^3 of an EO solution ($[\text{EO}] = 2.00 \times 10^{-5} \text{ mol dm}^{-3}$) with 20 sequential additions of a β -CD solution (50 mm^3 each, $[\beta\text{-CD}] = 3.04 \times 10^{-3} \text{ mol dm}^{-3}$) at 298.2 K . Both solutions were prepared in aqueous $\text{Na}_2\text{HPO}_4/\text{KH}_2\text{PO}_4$ buffer at $\text{pH } 7.0$ and $I = 0.10 \text{ mol dm}^{-3}$. The arrows indicate the direction of molar absorbance change with each addition of the β -CD solution. (Middle) Molar absorbance variation at 500 nm and the line representing the best-fit of an algorithm for a 1:1 host-guest complexation of EO by β -CD over the wavelength range $475\text{--}525 \text{ nm}$. (Bottom) Speciation plot with $[\text{EO}]_{\text{total}} = 100\%$ as the ratio $[\beta\text{-CD}]_{\text{total}}/[\text{EO}]_{\text{total}}$ increases.

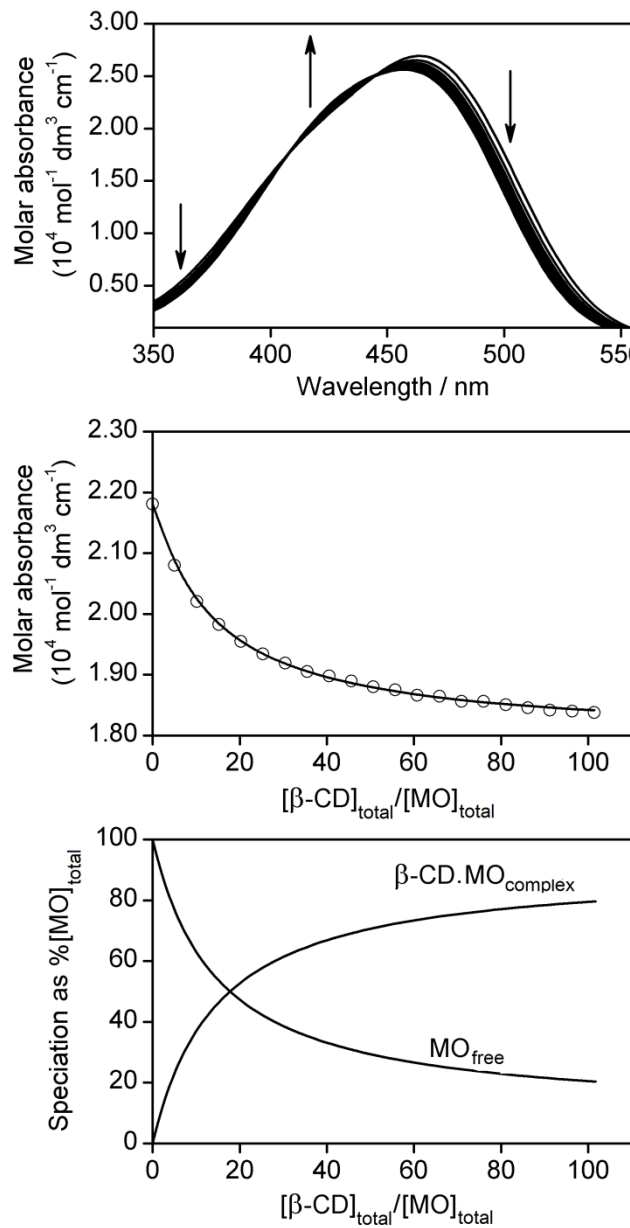


Figure S6: (Top) Molar absorbance variation of 1.5 cm^3 of a MO solution ($[\text{MO}] = 2.00 \times 10^{-5} \text{ mol dm}^{-3}$) with 20 sequential additions of a $\beta\text{-CD}$ solution (50 mm^3 each, $[\beta\text{-CD}] = 3.04 \times 10^{-3} \text{ mol dm}^{-3}$) at 298.2 K . Both solutions were prepared in aqueous $\text{Na}_2\text{HPO}_4/\text{KH}_2\text{PO}_4$ buffer at $\text{pH} 7.0$ and $I = 0.10 \text{ mol dm}^{-3}$. The arrows indicate the direction of molar absorbance variation with each addition of the $\beta\text{-CD}$ solution. (Middle) Molar absorbance variation at 490 nm and the line representing the best-fit of an algorithm for a 1:1 host–guest complexation of MO by $\beta\text{-CD}$ over the wavelength range $465\text{--}515 \text{ nm}$. (Bottom) Speciation plot with $[\text{MO}]_{\text{total}} = 100\%$ as the ratio $[\beta\text{-CD}]_{\text{total}}/[\text{MO}]_{\text{total}}$ increases.

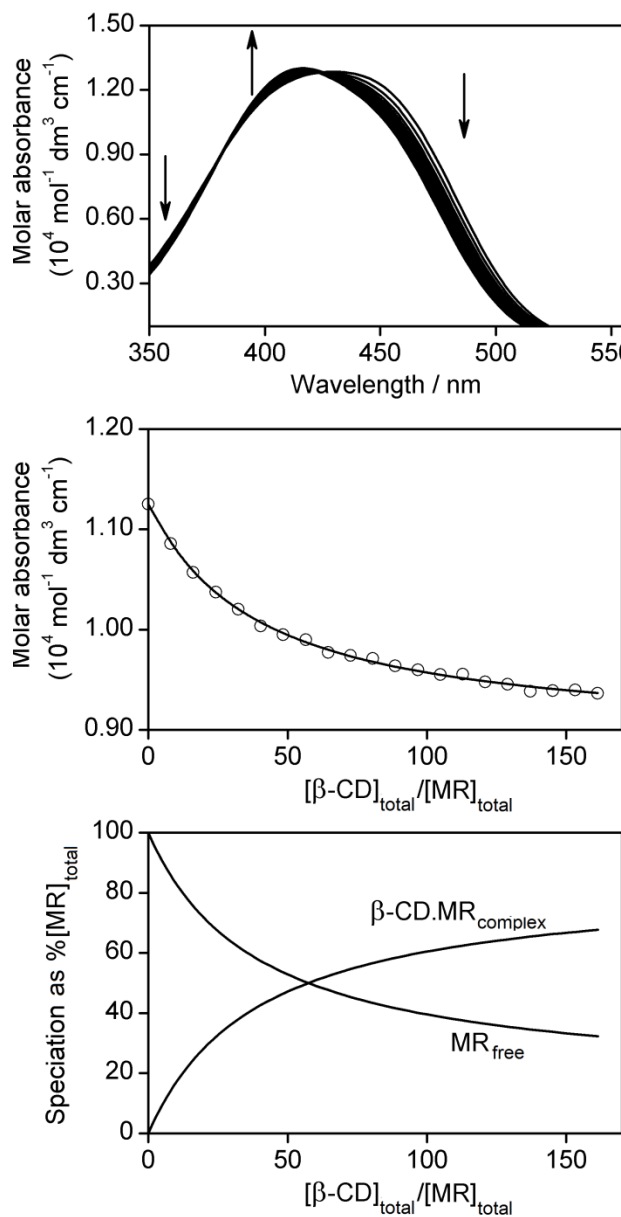


Figure S7: (Top) Molar absorbance variation of 1.5 cm^3 of a solution of MR ($[\text{MR}] = 2.80 \times 10^{-5} \text{ mol dm}^{-3}$) with 20 sequential additions of a β -CD solution (50 mm^3 each, $[\beta\text{-CD}] = 6.77 \times 10^{-3} \text{ mol dm}^{-3}$) at 298.2 K . Both solutions were prepared in aqueous $\text{Na}_2\text{HPO}_4/\text{KH}_2\text{PO}_4$ buffer at $\text{pH} 7.0$ and $I = 0.10 \text{ mol dm}^{-3}$. The arrows indicate the direction of molar absorbance change with each addition of the β -CD solution. (Middle) Molar absorbance variation at 460 nm and the line representing the best-fit of an algorithm for a 1:1 host–guest complexation of MR by β -CD over the wavelength range 430 – 480 nm . (Bottom) Speciation plot with $[\text{MR}]_{\text{total}} = 100\%$ as the ratio $[\beta\text{-CD}]_{\text{total}}/[\text{MR}]_{\text{total}}$ increases.

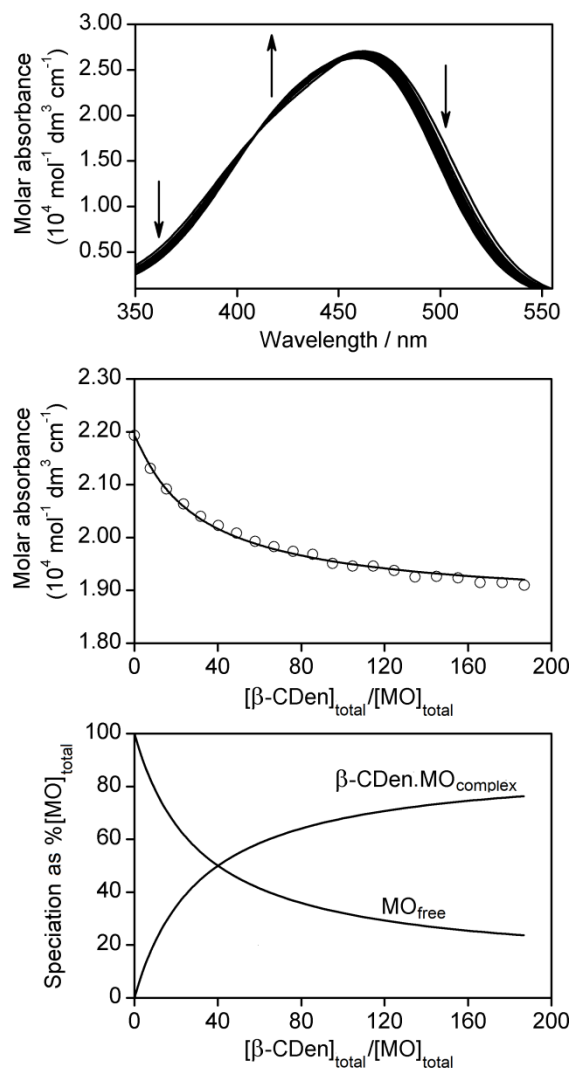


Figure S8: (Top) Molar absorbance variation of a MO solution ($[MO] = 2.00 \times 10^{-5} \text{ mol dm}^{-3}$) upon 20 sequential additions of a PAA β -CDen solution (50 mm^3 each, 0.98 wt %, $[\beta\text{-CDen substituents}] = 4.50 \times 10^{-3} \text{ mol dm}^{-3}$) at 298.2 K. Both solutions were prepared in aqueous $\text{Na}_2\text{HPO}_4/\text{KH}_2\text{PO}_4$ buffer at pH 7.0 and $I = 0.10 \text{ mol dm}^{-3}$. The arrows indicate the direction of molar absorbance variation upon each addition of the PAA β -CDen solution. (Middle) Molar absorbance variation at 490 nm and the line representing the best-fit of an algorithm for a 1:1 host–guest complexation of MO by β -CDen substituents of PAA β -CDen over the wavelength range 465–515 nm. (Bottom) Speciation plot with $[\text{MO}]_{\text{total}} = 100\%$ as the ratio $[\beta\text{-CDen}]_{\text{total}}/[\text{MO}]_{\text{total}}$ increases.

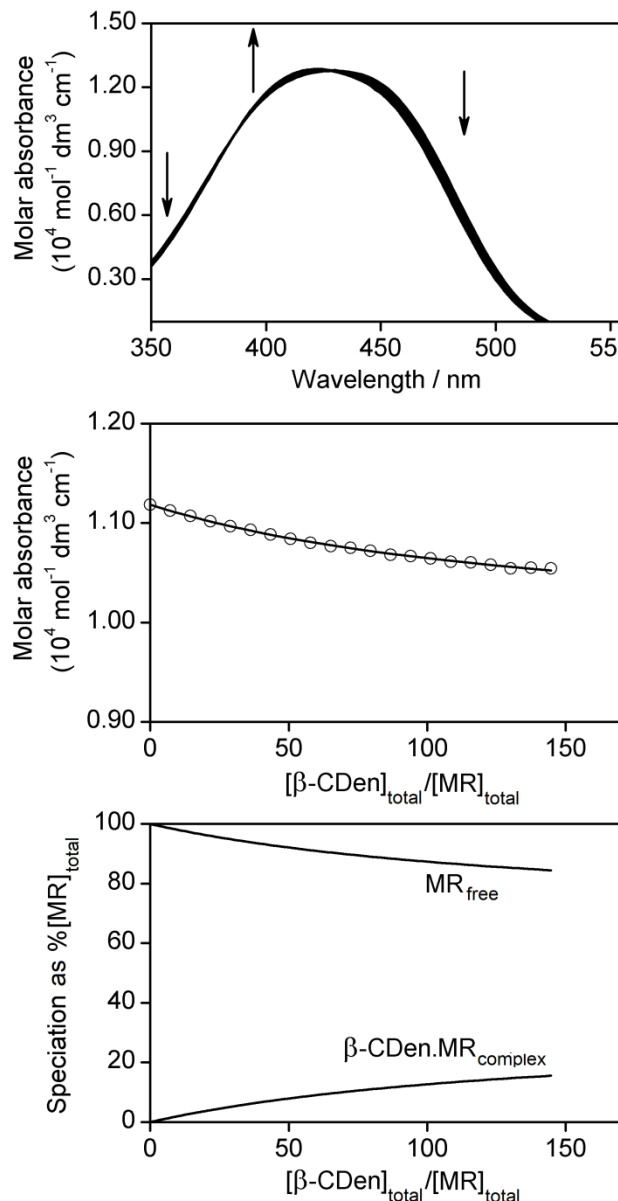


Figure S9: (Top) Molar absorbance variation of a MR solution ($[\text{MR}] = 2.80 \times 10^{-5} \text{ mol dm}^{-3}$) with 20 sequential additions of a PAA β -CDen solution (50 mm^3 each, 1.32 wt %, $[\beta\text{-CDen}] = 6.10 \times 10^{-3} \text{ mol dm}^{-3}$) at 298.2 K. Both solutions were prepared in aqueous $\text{Na}_2\text{HPO}_4/\text{KH}_2\text{PO}_4$ buffer at pH 7.0 and $I = 0.10 \text{ mol dm}^{-3}$. The arrows indicate the direction of molar absorbance variation with each addition of the PAA β -CDen solution. (Middle) Molar absorbance variation at 460 nm and the line representing the best-fit of an algorithm for a 1:1 host–guest complexation of MR by β -CDen substituents of PAA β -CDen over the wavelength range 430–480 nm. (Bottom) Speciation plot with $[\text{MR}]_{\text{total}} = 100\%$ as the ratio $[\beta\text{-CDen}]_{\text{total}}/[\text{MR}]_{\text{total}}$ increases.

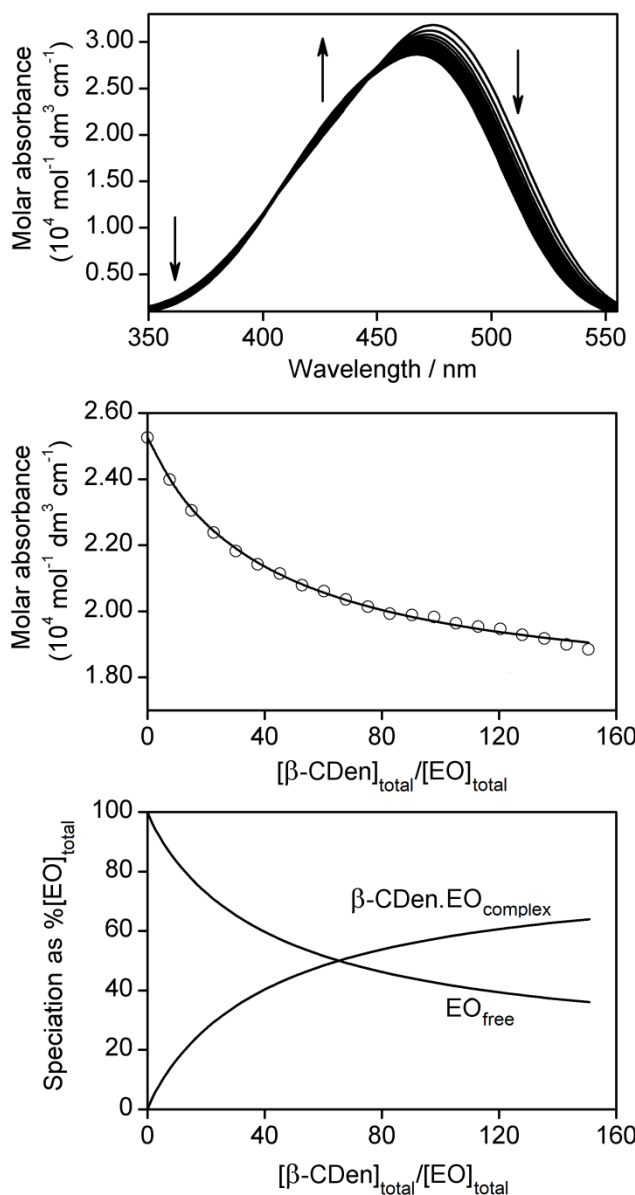


Figure S10: (Top) Molar absorbance variation of a 1.5 cm^3 of a solution of EO ($[\text{EO}] = 2.00 \times 10^{-5} \text{ mol dm}^{-3}$) with 20 sequential additions of a PAA β -CDen solution (25 mm^3 each, 1.93 wt %, $[\beta\text{-CDen}] = 9.03 \times 10^{-3} \text{ mol dm}^{-3}$) and a PAAADen solution (25 mm^3 each, 0.91 wt %, $[\text{ADen}] = 3.09 \times 10^{-3} \text{ mol dm}^{-3}$) at 298.2 K . All solutions were prepared in aqueous $\text{Na}_2\text{HPO}_4/\text{KH}_2\text{PO}_4$ buffer solutions at $\text{pH} 7.0$ and $I = 0.10 \text{ mol dm}^{-3}$. The arrows indicate the direction of molar absorbance variation with each addition of the PAA β -CDen and PAAADen solutions. (Middle) Molar absorbance variation at 500 nm and the line representing the best-fit of an algorithm for a 1:1 host–guest complexation of EO by β -CDen substituents in self-assembled PAA β -CDen/PAAADen network over the wavelength range 475 – 525 nm . (Bottom) Speciation plot with $[\text{EO}]_{\text{total}} = 100\%$ as the $[\beta\text{-CDen}]_{\text{total}}/[\text{EO}]_{\text{total}}$ increases.

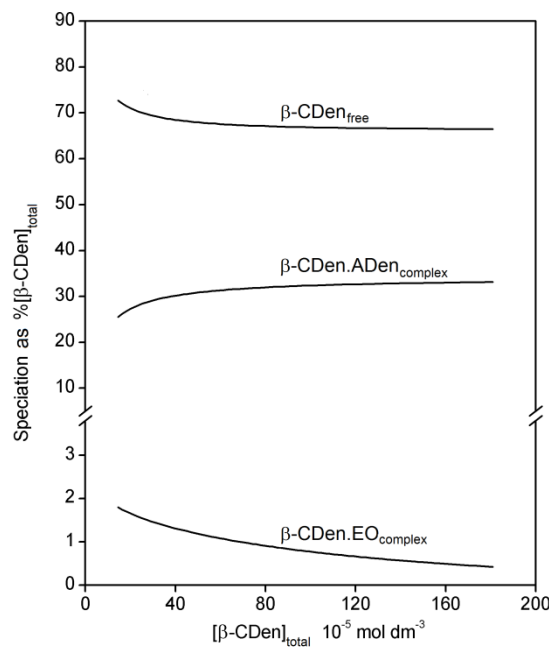


Figure S11: Speciation plot with $[\beta\text{-CDen}]_{\text{total}} = 100\%$ for the PAA β -CDen/PAAADen/EO system.

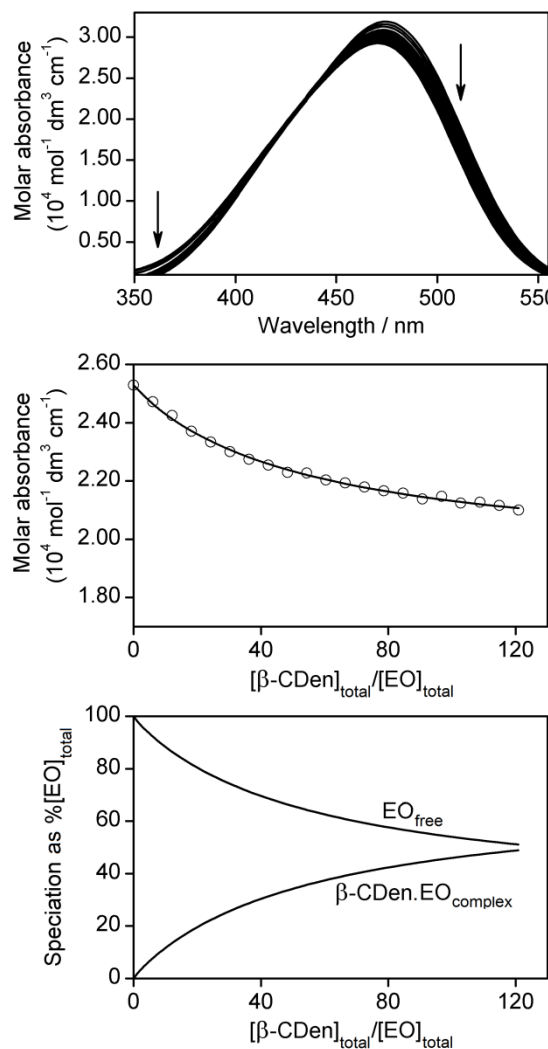


Figure S12: (Top) Molar absorbance variation of 1.5 cm^3 of a solution of EO ($[\text{EO}] = 2.00 \times 10^{-5} \text{ mol dm}^{-3}$) with 20 sequential additions of a PAA β -CDen solution (25 mm^3 each, 1.56 wt %, $[\beta\text{-CDen}] = 7.26 \times 10^{-3} \text{ mol dm}^{-3}$) and a PAAADddn solution (25 mm^3 each, 0.85 wt %, $[\text{ADddn}] = 2.43 \times 10^{-3} \text{ mol dm}^{-3}$) at 298.2 K . All solutions were prepared in aqueous $\text{Na}_2\text{HPO}_4/\text{KH}_2\text{PO}_4$ buffer at $\text{pH} 7.0$ and $I = 0.10 \text{ mol dm}^{-3}$. The arrows indicate the direction of molar absorbance variation with each addition of the PAA β -CDen and PAAADddn solutions. (Middle) Molar absorbance variation at 500 nm and the line representing the best-fit of an algorithm for a 1:1 host–guest complexation of EO by β -CDen substituents in self-assembled PAA β -CDen/PAAADddn network over the wavelength range 475 – 525 nm . (Bottom) Speciation plot with $[\text{EO}]_{\text{total}} = 100\%$ as the $[\beta\text{-CDen}]_{\text{total}}/[\text{EO}]_{\text{total}}$ increases.

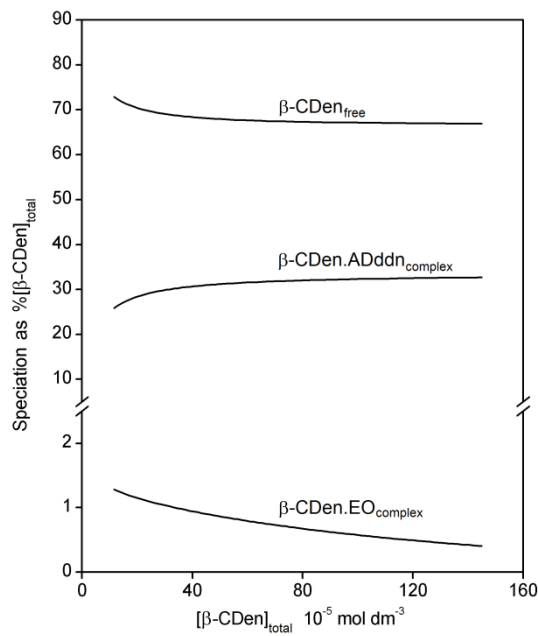


Figure S13: Speciation plot with $[\beta\text{-CDen}]_{\text{total}} = 100\%$ for PAA β -CDen/PAAADddn/EO system.

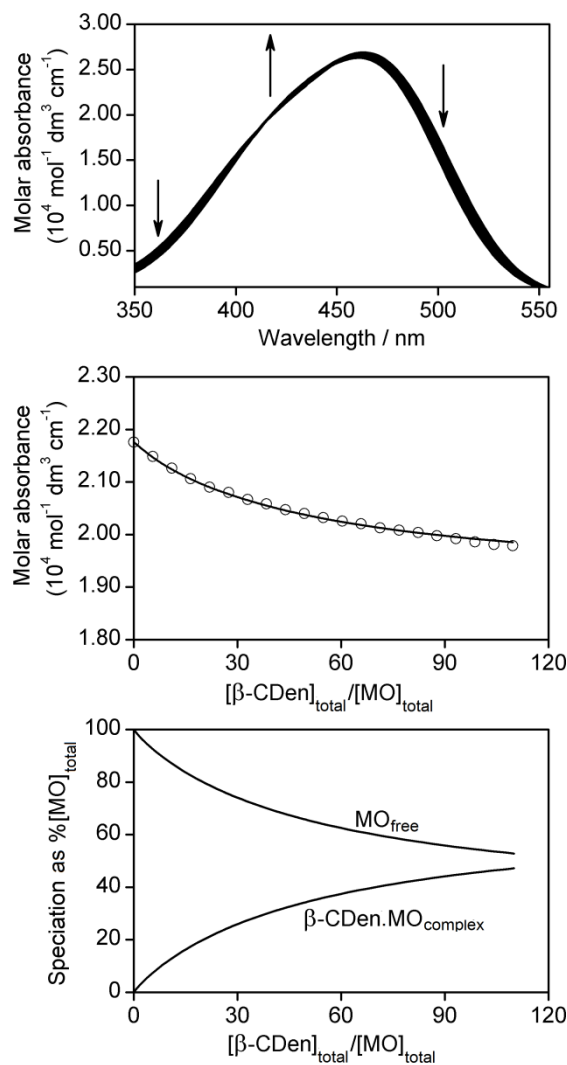


Figure S14: (Top) Molar absorbance variation of 1.5 cm^3 of a solution of MO ($[\text{MO}] = 2.00 \times 10^{-5} \text{ mol dm}^{-3}$) upon 20 sequential additions of a PAA β -CDen solution (25 mm^3 each, 1.42 wt %, $[\beta\text{-CDen}] = 6.58 \times 10^{-3} \text{ mol dm}^{-3}$) and a PAAADen solution (25 mm^3 each, 0.65 wt %, [ADen substituents] = $2.19 \times 10^{-3} \text{ mol dm}^{-3}$) at 298.2 K . All solutions were prepared in aqueous $\text{Na}_2\text{HPO}_4/\text{KH}_2\text{PO}_4$ buffer solutions at $\text{pH} 7.0$ and $I = 0.10 \text{ mol dm}^{-3}$. The arrows indicate the direction of molar absorbance variation upon each addition of the PAA β -CDen and PAAADen solutions. (Middle) Molar absorbance variation at 490 nm and the line representing the best-fit of an algorithm for a 1:1 host–guest complexation of MO by β -CDen substituents in self-assembled PAA β -CDen/PAAADen network over the wavelength range $465\text{--}515 \text{ nm}$. (Bottom) Speciation plot with $[\text{MO}]_{\text{total}} = 100\%$ as the $[\beta\text{-CDen}]_{\text{total}}/[\text{EO}]_{\text{total}}$ increases.

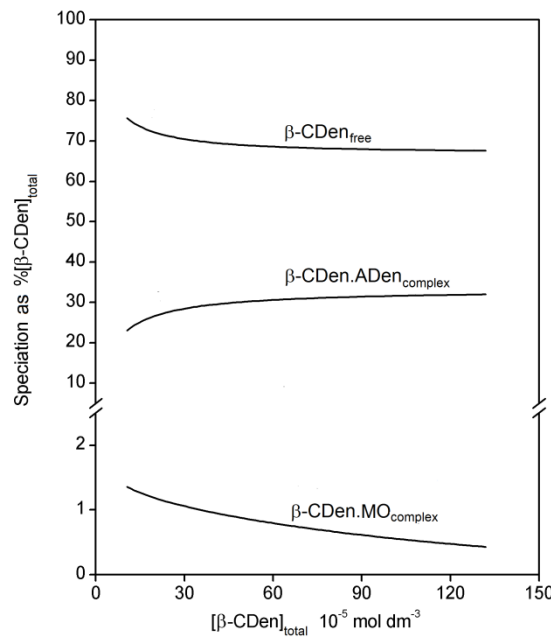


Figure S15: Speciation plot with $[\beta\text{-CDen}]_{\text{total}} = 100\%$ for the PAA β -CDen/PAAADen/MO system.

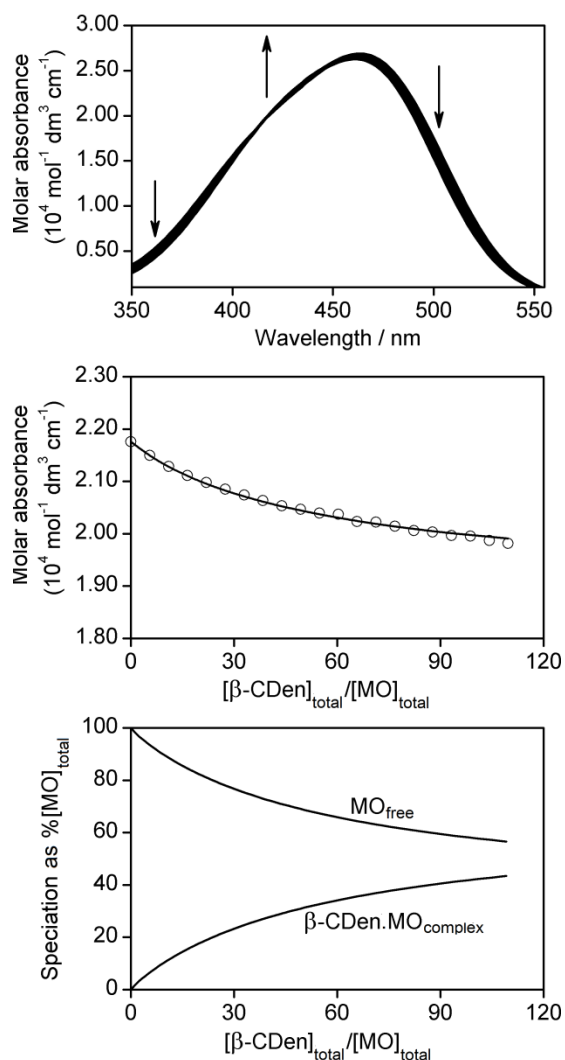


Figure S16: (Top) Molar absorbance variation of 1.5 cm^3 of a solution of MO ($[\text{MO}] = 2.00 \times 10^{-5} \text{ mol dm}^{-3}$) with 20 sequential additions of a PAA β -CDen solution (25 mm^3 each, 1.42 wt %, $[\beta\text{-CDen}] = 6.58 \times 10^{-3} \text{ mol dm}^{-3}$) and a PAAADhn solution (25 mm^3 each, 0.74 wt %, $[\text{ADhn}] = 2.23 \times 10^{-3} \text{ mol dm}^{-3}$) at 298.2 K. All solutions were prepared in aqueous $\text{Na}_2\text{HPO}_4/\text{KH}_2\text{PO}_4$ buffer at pH 7.0 and $I = 0.10 \text{ mol dm}^{-3}$. The arrows indicate the direction of molar absorbance variation with each addition of the PAA β -CDen and PAAADhn solutions. (Middle) Molar absorbance variation at 490 nm and the line representing the best-fit of an algorithm for a 1:1 host–guest complexation of MO by β -CDen substituents in self-assembled PAA β -CDen/PAAADhn network over the wavelength range 465–515 nm. (Bottom) Speciation plot with $[\text{MO}]_{\text{total}} = 100\%$ as the $[\beta\text{-CDen}]_{\text{total}}/[\text{MO}]_{\text{total}}$ increases.

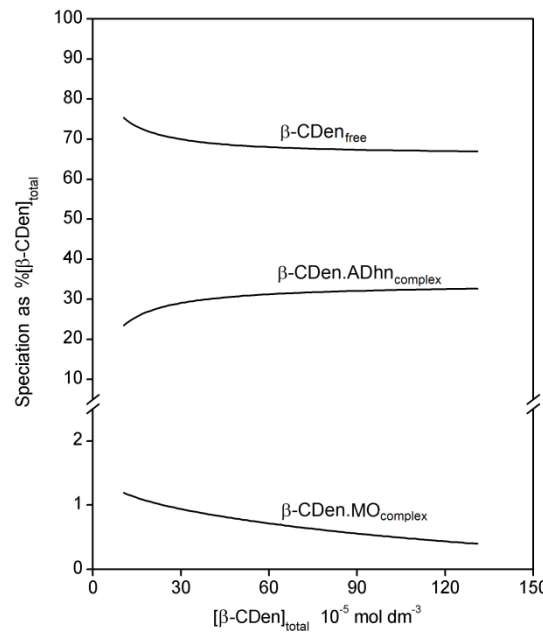


Figure S17: Speciation plot with $[\beta\text{-CDen}]_{\text{total}} = 100\%$ for the PAA β -CDen/PAAADhn/MO system.

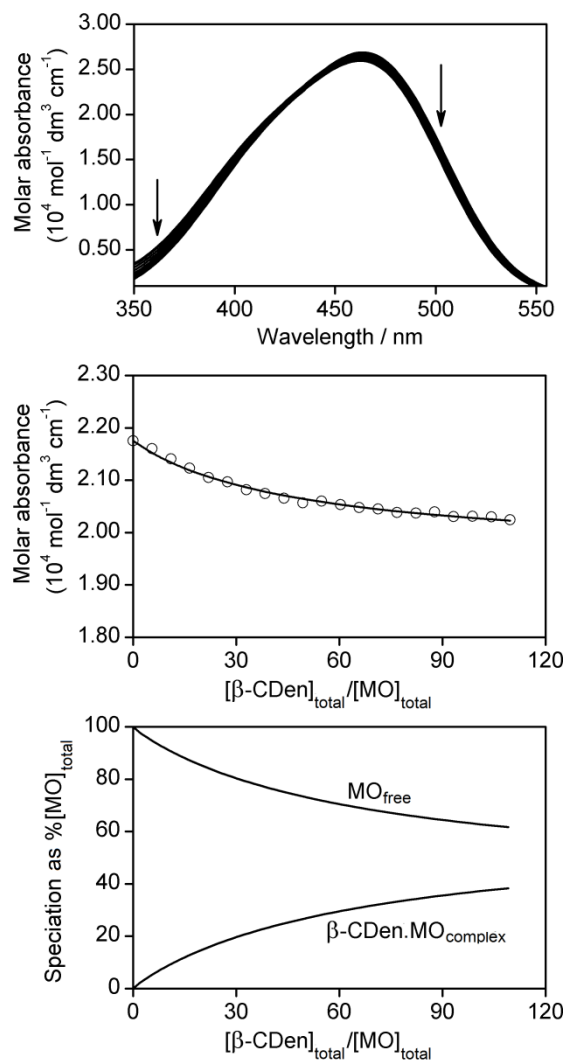


Figure S18: (Top) Molar absorbance variation of 1.5 cm^3 of a solution of MO ($[\text{MO}] = 2.00 \times 10^{-5} \text{ mol dm}^{-3}$) with 20 sequential additions of a PAA β -CDen solution (25 mm^3 each, 1.42 wt %, $[\beta\text{-CDen}] = 6.58 \times 10^{-3} \text{ mol dm}^{-3}$) and a PAAADddn solution (25 mm^3 each, 0.78 wt %, $[\text{ADddn}] = 2.23 \times 10^{-3} \text{ mol dm}^{-3}$) at 298.2 K . All solutions were prepared in aqueous $\text{Na}_2\text{HPO}_4/\text{KH}_2\text{PO}_4$ buffer at $\text{pH} 7.0$ and $I = 0.10 \text{ mol dm}^{-3}$. The arrows indicate the direction of molar absorbance variation each addition of the PAA β -CDen and PAAADddn solutions. (Middle) Molar absorbance variation at 490 nm and the line representing the best-fit of an algorithm for a 1:1 host–guest complexation of MO by β -CDen substituents in self-assembled PAA β -CDen/PAAADddn network over the wavelength range 465 – 515 nm . (Bottom) Speciation plot with $[\text{MO}]_{\text{total}} = 100\%$ as the $[\beta\text{-CDen}]_{\text{total}}/[\text{MO}]_{\text{total}}$ increases.

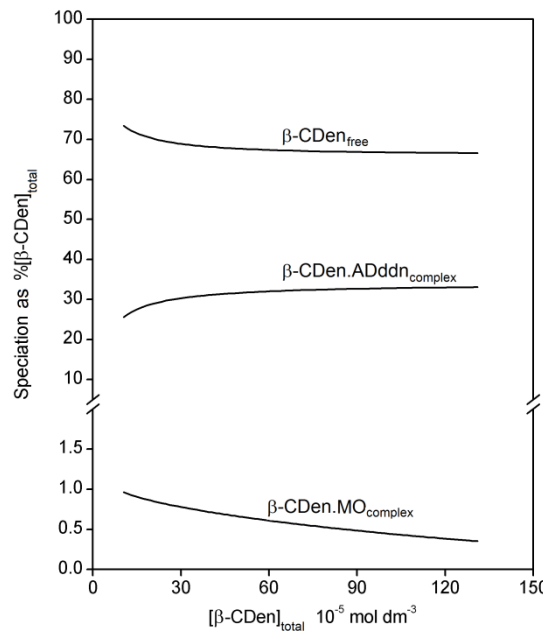


Figure S19: Speciation plot with $[\beta\text{-CDen}]_{\text{total}} = 100\%$ for the PAA β -CDen/PAAADddn/MO system.

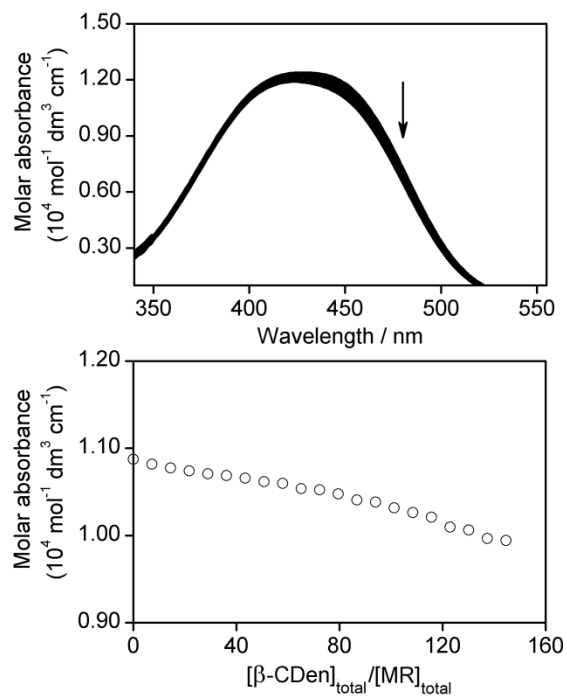


Figure S20: (Top) Molar absorbance variation of 1.5 cm^3 of a solution of MR ($[\text{MR}] = 2.80 \times 10^{-5} \text{ mol dm}^{-3}$) with 20 sequential additions of a $\text{PAA}\beta\text{-CDen}$ solution (25 mm^3 each, 2.59 wt %, $[\beta\text{-CDen}] = 1.22 \times 10^{-2} \text{ mol dm}^{-3}$) and a PAAADen solution (25 mm^3 each, 1.18 wt %, $[\text{ADen}] = 4.03 \times 10^{-3} \text{ mol dm}^{-3}$) at 298.2 K . All solutions were prepared in aqueous $\text{Na}_2\text{HPO}_4/\text{KH}_2\text{PO}_4$ buffer at $\text{pH} 7.0$ and $I = 0.10 \text{ mol dm}^{-3}$. The arrow indicates the direction of molar absorbance variation with each addition of the $\text{PAA}\beta\text{-CDen}$ and PAAADen solutions. (Bottom) Molar absorbance variation at 460 nm is insufficient to fit to an algorithm for host-guest complexation of MR by $\beta\text{-CDen}$ in the self-assembled $\text{PAA}\beta\text{-CDen}/\text{PAAADen}$ network.

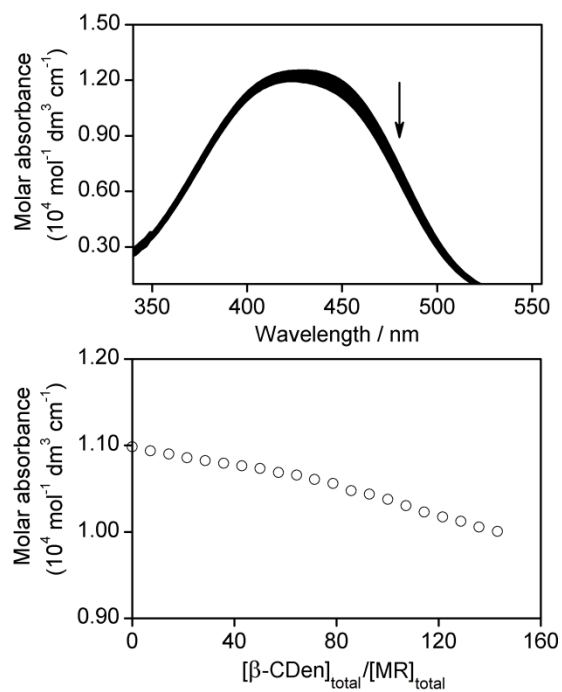


Figure S21: (Top) Molar absorbance variation 1.5 cm^3 of a solution of MR ($[\text{MR}] = 2.80 \times 10^{-5} \text{ mol dm}^{-3}$) with 20 sequential additions of a $\text{PAA}\beta\text{-CDen}$ solution (25 mm^3 each, 2.54 wt %, $[\beta\text{-CDen}] = 1.20 \times 10^{-2} \text{ mol dm}^{-3}$) and a PAAADhn solution (25 mm^3 each, 1.30 wt %, $[\text{ADhn}] = 4.00 \times 10^{-3} \text{ mol dm}^{-3}$) at 298.2 K . All solutions were prepared in aqueous $\text{Na}_2\text{HPO}_4/\text{KH}_2\text{PO}_4$ buffer at $\text{pH} 7.0$ and $I = 0.10 \text{ mol dm}^{-3}$. The arrow indicates the direction of molar absorbance variation with each addition of the $\text{PAA}\beta\text{-CDen}$ and PAAADhn solutions. (Bottom) Molar absorbance variation at 460 nm is insufficient to fit to an algorithm for host-guest complexation of MR by $\beta\text{-CDen}$ in the self-assembled $\text{PAA}\beta\text{-CDen}/\text{PAAADhn}$ network.

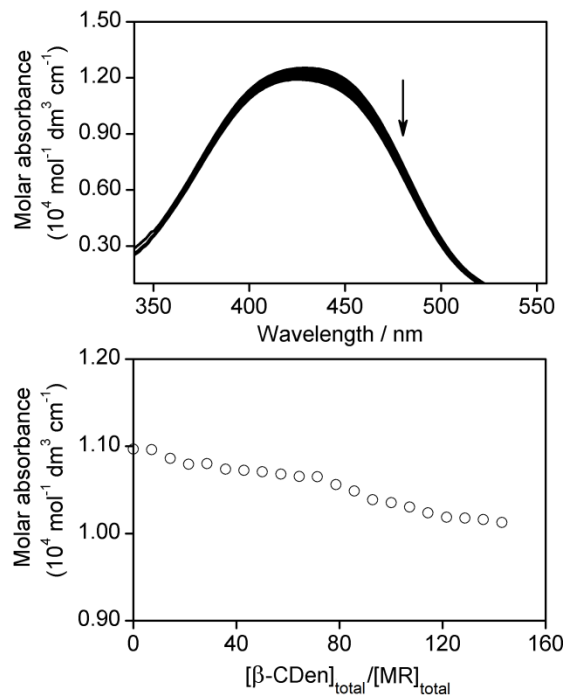


Figure S22: (Top) Molar absorbance variation of 1.5 cm^3 of a solution of MR ($[\text{MR}] = 2.80 \times 10^{-5}\text{ mol dm}^{-3}$) with 20 sequential additions of a $\text{PAA}\beta\text{-CDen}$ solution (25 mm^3 each, 2.54 wt %, $[\beta\text{-CDen}] = 1.20 \times 10^{-2}\text{ mol dm}^{-3}$) and a PAAADddn solution (25 mm^3 each, 1.37 wt %, $[\text{ADddn}] = 4.01 \times 10^{-3}\text{ mol dm}^{-3}$) at 298.2 K . All solutions were prepared in aqueous $\text{Na}_2\text{HPO}_4/\text{KH}_2\text{PO}_4$ buffer at $\text{pH } 7.0$ and $I = 0.10\text{ mol dm}^{-3}$. The arrow indicates the direction of molar absorbance variation with each addition of the $\text{PAA}\beta\text{-CDen}$ and PAAADddn solutions. (Bottom) Molar absorbance variation at 460 nm is insufficient to fit to an algorithm for host-guest complexation of MR by $\beta\text{-CDen}$ in the self-assembled $\text{PAA}\beta\text{-CDen}/\text{PAAADddn}$ network.

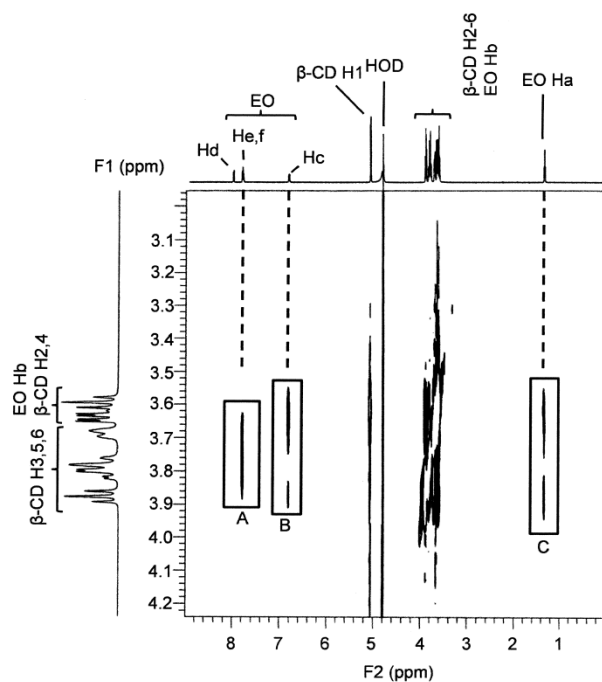


Figure S23: 2D ROESY ^1H NMR spectrum of EO ($[\text{EO}] = 2.0 \times 10^{-3} \text{ mol dm}^{-3}$) and $\beta\text{-CD}$ ($[\beta\text{-CD}] = 2.0 \times 10^{-3} \text{ mol dm}^{-3}$) in D_2O $\text{Na}_2\text{HPO}_4/\text{KH}_2\text{PO}_4$ buffer solution at $\text{pD} = 7.0$ and $I = 0.10 \text{ mol dm}^{-3}$ at 298.2 K . Cross-peaks in boxes A, B, and C arise from dipolar interactions between the $\beta\text{-CD}$ annular $\text{H}3,5,6$ protons and the EO aromatic (Hc, He and Hf) and methyl (Ha) protons, respectively. Dipolar interactions between EO methylene (Hb) protons and adjacent aromatic (Hc) and methyl (Ha) protons of EO, respectively, also contribute to the cross-peaks in boxes B and C, respectively.

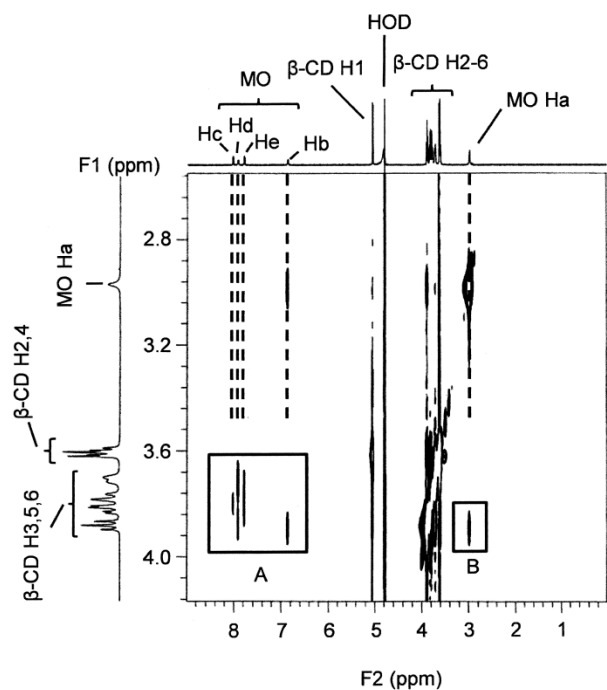


Figure S24: 2D ROESY ^1H NMR spectrum of MO ($[\text{MO}] = 2.0 \times 10^{-3} \text{ mol dm}^{-3}$) and $\beta\text{-CD}$ ($[\beta\text{-CD}] = 2.0 \times 10^{-3} \text{ mol dm}^{-3}$) in D_2O $\text{Na}_2\text{HPO}_4/\text{KH}_2\text{PO}_4$ buffer solution at $\text{pD} = 7.0$ and $I = 0.10 \text{ mol dm}^{-3}$ at 298.2 K . Cross-peaks in boxes A and B arise from dipolar interactions between the $\beta\text{-CD}$ annular H3,5,6 protons and the aromatic (Hb–e) and methyl (Ha) protons of MO, respectively.

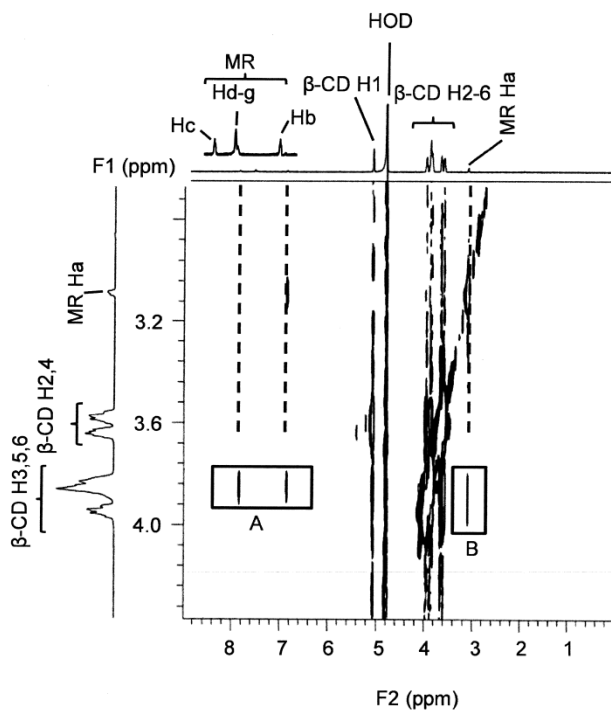


Figure S25: 2D ROESY ^1H NMR spectrum of MR ($[\text{MR}] = 2.0 \times 10^{-3} \text{ mol dm}^{-3}$) and $\beta\text{-CD}$ ($[\beta\text{-CD}] = 2.0 \times 10^{-3} \text{ mol dm}^{-3}$) in D_2O $\text{Na}_2\text{HPO}_4/\text{KH}_2\text{PO}_4$ buffer solution at $\text{pD} = 7.0$ and $I = 0.10 \text{ mol dm}^{-3}$ at 298.2 K . Cross-peaks in boxes A and B arise from dipolar interactions between the $\beta\text{-CD}$ annular $\text{H}_{3,5,6}$ protons and the aromatic (Hb and Hc) and methyl (Ha) protons of MR, respectively.

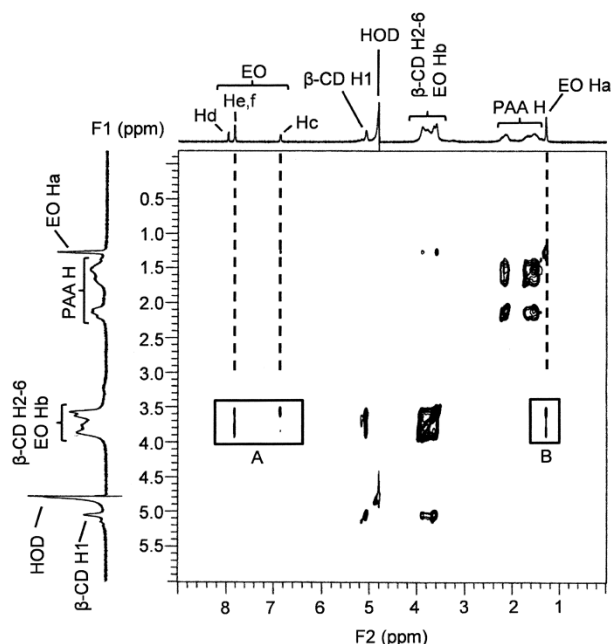


Figure S26: 2D NOESY ^1H NMR spectrum of EO ($[\text{EO}] = 2.0 \times 10^{-3} \text{ mol dm}^{-3}$) and $\text{PAA}\beta\text{-CDen}$ (0.44 wt %, $[\beta\text{-CDen}] = 2.0 \times 10^{-3} \text{ mol dm}^{-3}$) in D_2O $\text{Na}_2\text{HPO}_4/\text{KH}_2\text{PO}_4$ buffer solution at $\text{pD} = 7.0$ and $I = 0.10 \text{ mol dm}^{-3}$ at 298.2 K . Cross-peaks in boxes A and B arise from dipolar interactions between the annular $\text{H}_{3,5,6}$ protons of $\beta\text{-CDen}$ and the aromatic (Hc, He and Hf) and methyl (Ha) protons of EO, respectively.

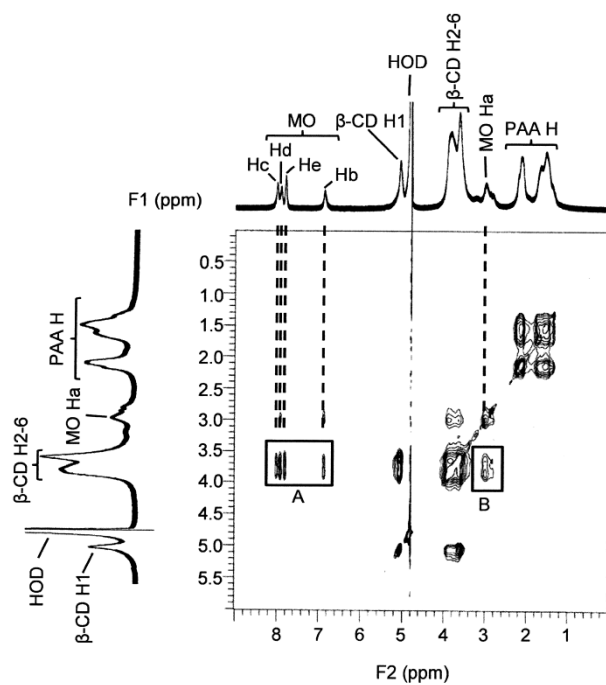


Figure S27: 2D NOESY ^1H NMR spectrum of MO ($[\text{MO}] = 2.0 \times 10^{-3} \text{ mol dm}^{-3}$) and PAA β -CDen (0.44 wt %, $[\beta\text{-CDen}] = 2.0 \times 10^{-3} \text{ mol dm}^{-3}$) in D_2O $\text{Na}_2\text{HPO}_4/\text{KH}_2\text{PO}_4$ buffer solution at $\text{pD} = 7.0$ and $I = 0.10 \text{ mol dm}^{-3}$ at 298.2 K. Cross-peaks in boxes A and B arise from dipolar interactions between the annular H3,5,6 protons of β -CDen and the aromatic (Hb–e) and methyl (Ha) protons of MO, respectively.

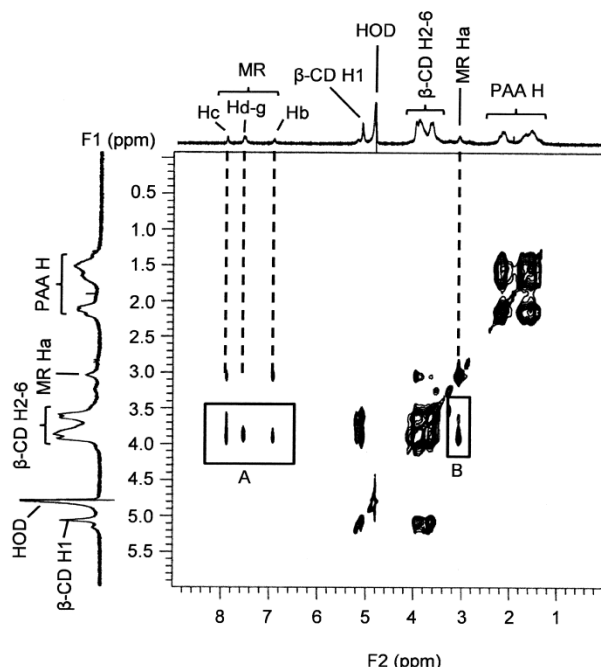


Figure S28: 2D NOESY ^1H NMR spectrum of MR ($[\text{MR}] = 2.0 \times 10^{-3} \text{ mol dm}^{-3}$) and PAA β -CDen (0.44 wt %, $[\beta\text{-CDen}] = 2.0 \times 10^{-3} \text{ mol dm}^{-3}$) in D_2O $\text{Na}_2\text{HPO}_4/\text{KH}_2\text{PO}_4$ buffer solution at $\text{pD} = 7.0$ and $I = 0.10 \text{ mol dm}^{-3}$ at 298.2 K. Cross-peaks in boxes A and B arise from dipolar interactions between the annular H3,5,6 protons of β -CDen and the aromatic (Hb–g) and methyl (Ha) protons of MR, respectively.

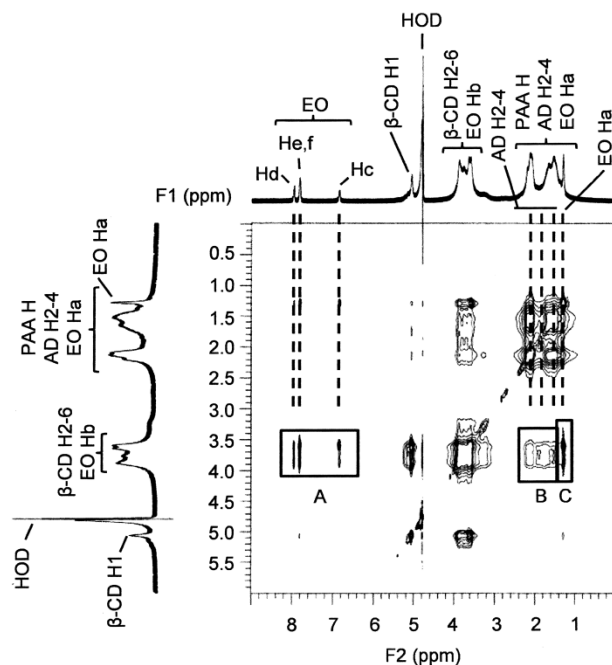


Figure S29: 2D NOESY ^1H NMR spectrum of EO ($[\text{EO}] = 2.0 \times 10^{-3} \text{ mol dm}^{-3}$) and PAA β -CDen (0.78 wt %, $[\beta\text{-CDen}] = 3.6 \times 10^{-3} \text{ mol dm}^{-3}$) and PAAADen (0.36 wt %, $[\text{ADen}] = 1.2 \times 10^{-3} \text{ mol dm}^{-3}$) in D_2O $\text{Na}_2\text{HPO}_4/\text{KH}_2\text{PO}_4$ buffer solution at $\text{pD} = 7.0$ and $I = 0.10 \text{ mol dm}^{-3}$ at 298.2 K. Cross-peaks in boxes A and C arise from dipolar interactions between the annular H3,5,6 protons of β -CDen and the aromatic (Hc–f) and methyl (Ha) protons of EO, respectively. Cross-peaks in box B arise from dipolar interactions between the annular H3,5,6 protons of β -CDen and the H2–4 protons of ADen.

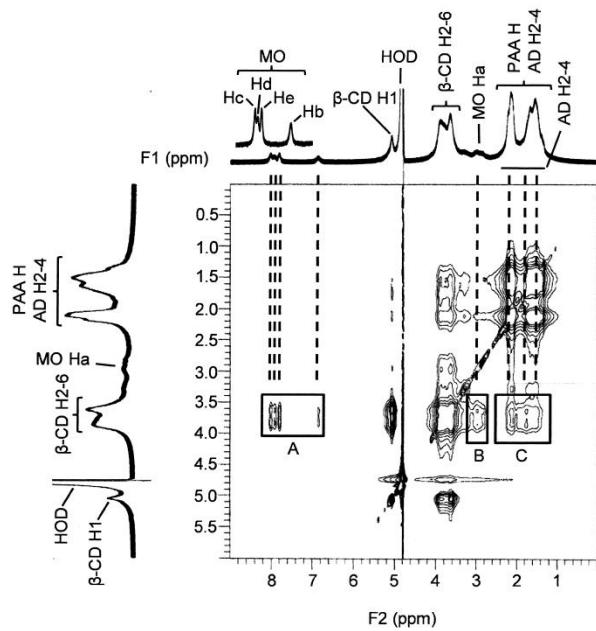


Figure S30: 2D NOESY ^1H NMR spectrum of MO ($[\text{MO}] = 2.0 \times 10^{-3} \text{ mol dm}^{-3}$) and PAA β -CDen (0.78 wt %, $[\beta\text{-CDen}] = 3.6 \times 10^{-3} \text{ mol dm}^{-3}$) and PAAADen (0.36 wt %, $[\text{ADen}] = 1.2 \times 10^{-3} \text{ mol dm}^{-3}$) in D_2O $\text{Na}_2\text{HPO}_4/\text{KH}_2\text{PO}_4$ buffer solution at $\text{pD} = 7.0$ and $I = 0.10 \text{ mol dm}^{-3}$ at 298.2 K. Cross-peaks in boxes A and C arise from dipolar interactions between the annular H3,5,6 protons of β -CDen and the aromatic (Hb–e) and methyl (Ha) protons of MO, respectively. Cross-peaks in box B arise from dipolar interactions between the annular H3,5,6 protons of β -CDen and the H2–4 protons of ADen.

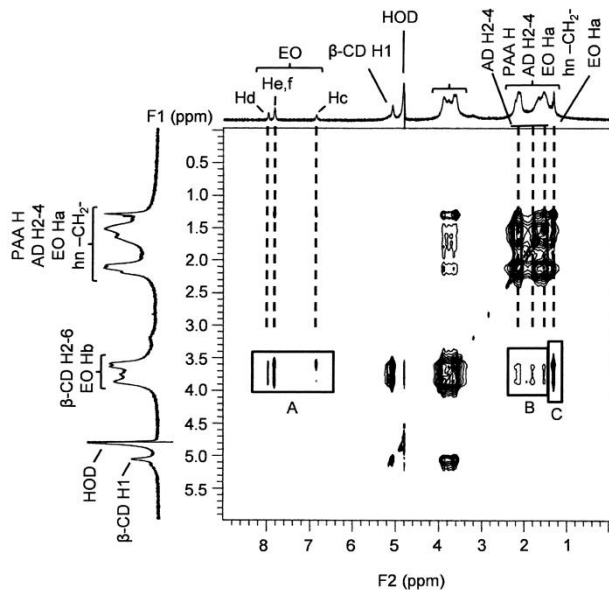


Figure S31: 2D NOESY ^1H NMR spectrum of EO ($[\text{EO}] = 2.0 \times 10^{-3}$ mol dm^{-3}) and PAA β -CDen (0.78 wt %, $[\beta\text{-CDen}] = 3.6 \times 10^{-3}$ mol dm^{-3}) and PAAADhn (0.40 wt %, $[\text{ADhn}] = 1.2 \times 10^{-3}$ mol dm^{-3}) in D_2O $\text{Na}_2\text{HPO}_4/\text{KH}_2\text{PO}_4$ buffer solution at $\text{pD} = 7.0$ and $I = 0.10$ mol dm^{-3} at 298.2 K. Cross-peaks in boxes A and C arise from dipolar interactions between the annular H3,5,6 protons of β -CDen and the aromatic (Hc–f) and methyl (Ha) protons of EO, respectively. Cross-peaks in box B arise from dipolar interactions between the annular H3,5,6 protons of β -CD and the H2–4 protons of ADhn.

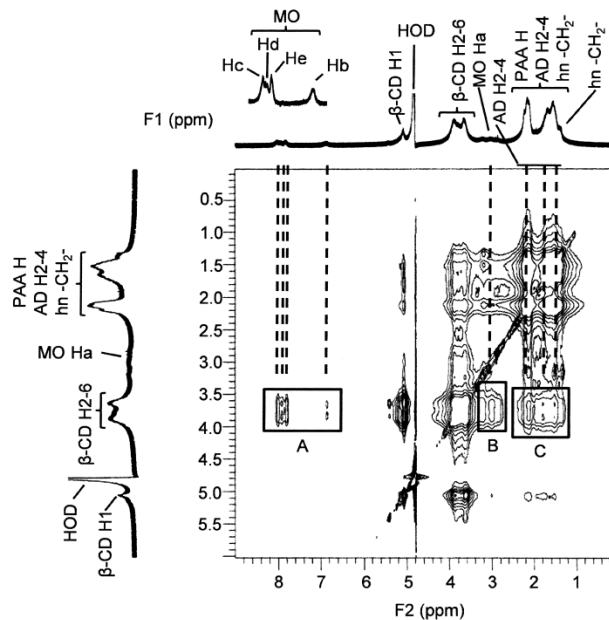


Figure S32: 2D NOESY ^1H NMR spectrum of MO ($[\text{MO}] = 2.0 \times 10^{-3}$ mol dm^{-3}) and PAA β -CDen (0.78 wt %, $[\beta\text{-CDen}] = 3.6 \times 10^{-3}$ mol dm^{-3}) and PAAADhn (0.40 wt %, $[\text{ADhn}] = 1.2 \times 10^{-3}$ mol dm^{-3}) in D_2O $\text{Na}_2\text{HPO}_4/\text{KH}_2\text{PO}_4$ buffer solution at $\text{pD} = 7.0$ and $I = 0.10$ mol dm^{-3} at 298.2 K. Cross-peaks in boxes A and B arise from dipolar interactions between the annular H3,5,6 protons of β -CDen and the aromatic (Hb–e) and methyl (Ha) protons of MO, respectively. Cross-peaks in box C arise from dipolar interactions between the annular H3,5,6 protons of β -CDen and the H2–4 protons of ADhn.

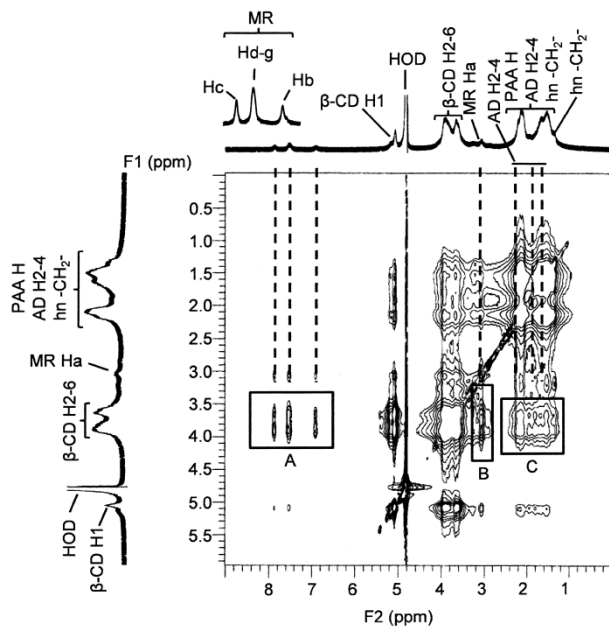


Figure S33: 2D NOESY ^1H NMR spectrum of MR ($[\text{MR}] = 2.0 \times 10^{-3} \text{ mol dm}^{-3}$) and PAA β -CDen ($0.78 \text{ wt } \%$, $[\beta\text{-CDen}] = 3.6 \times 10^{-3} \text{ mol dm}^{-3}$) and PAAADhn ($0.40 \text{ wt } \%$, $[\text{ADhn}] = 1.2 \times 10^{-3} \text{ mol dm}^{-3}$) in D_2O $\text{Na}_2\text{HPO}_4/\text{KH}_2\text{PO}_4$ buffer solution at $\text{pD} = 7.0$ and $I = 0.10 \text{ mol dm}^{-3}$ at 298.2 K . Cross-peaks in boxes A and B arise from dipolar interactions between the annular H3,5,6 protons of $[\beta\text{-CDen}$ and the aromatic (Hb-g) and methyl (Ha) protons of MR, respectively. Cross-peaks in box C arise from dipolar interactions between the annular H3,5,6 protons of $[\beta\text{-CDen}$ and the H2-4 protons of ADhn.

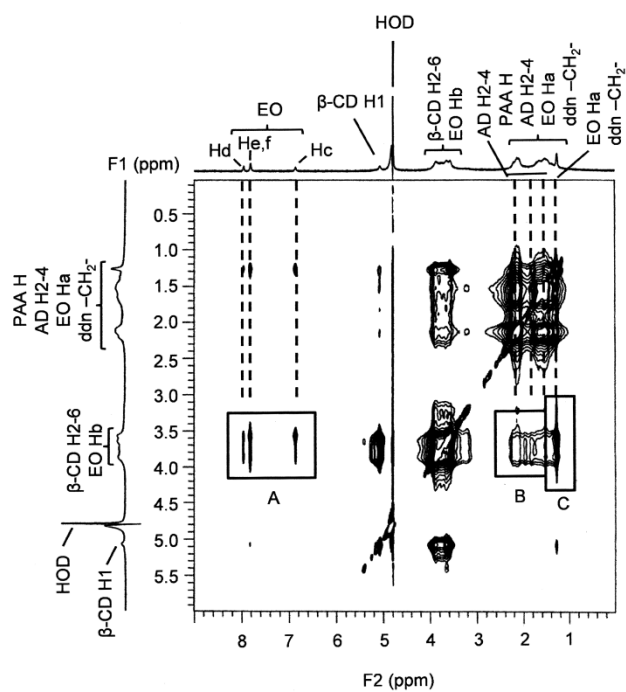


Figure S34: 2D NOESY ^1H NMR spectrum of EO ($[\text{EO}] = 2.0 \times 10^{-3} \text{ mol dm}^{-3}$) and PAA β -CDen (0.78 wt %, $[\beta\text{-CDen}] = 3.6 \times 10^{-3} \text{ mol dm}^{-3}$) and PAAADddn (0.42 wt %, $[\text{ADddn}] = 1.2 \times 10^{-3} \text{ mol dm}^{-3}$) in D_2O $\text{Na}_2\text{HPO}_4/\text{KH}_2\text{PO}_4$ buffer solution at $\text{pD} = 7.0$ and $I = 0.10 \text{ mol dm}^{-3}$ at 298.2 K. Cross-peaks in box A arise from dipolar interactions between the annular H3,5,6 protons of β -CDen and the aromatic (Hc–f) protons of EO. Cross-peaks in box B arise from dipolar interactions between the annular H3,5,6 protons of β -CDen and the H2–4 protons of ADddn. Cross-peaks in box C arise from dipolar interactions between the annular H3,5,6 protons of β -CDen and the tether dodecyl methylene protons of ADddn and the methyl (Ha) protons of EO.

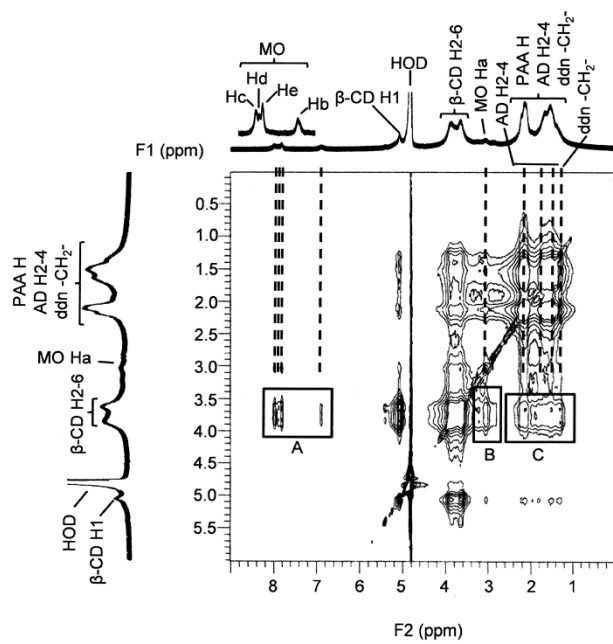


Figure S35: 2D NOESY ^1H NMR spectrum of MO ($[\text{MO}] = 2.0 \times 10^{-3} \text{ mol dm}^{-3}$) and PAA β -CDen (0.78 wt %, $[\beta\text{-CDen}] = 3.6 \times 10^{-3} \text{ mol dm}^{-3}$) and PAAADddn (0.42 wt %, $[\text{ADddn}] = 1.2 \times 10^{-3} \text{ mol dm}^{-3}$) in D_2O $\text{Na}_2\text{HPO}_4/\text{KH}_2\text{PO}_4$ buffer solution at $\text{pD} = 7.0$ and $I = 0.10 \text{ mol dm}^{-3}$ at 298.2 K. Cross-peaks in boxes A and B arise from dipolar interactions between the annular H3,5,6 protons of β -CDen and the aromatic (Hb–e) and methyl (Ha) protons of MO, respectively. Cross-peaks in box C arise from dipolar interactions between the annular H3,5,6 protons of β -CDen and the H2–4 protons of the ADddn groups and the tether dodecyl methylene protons.

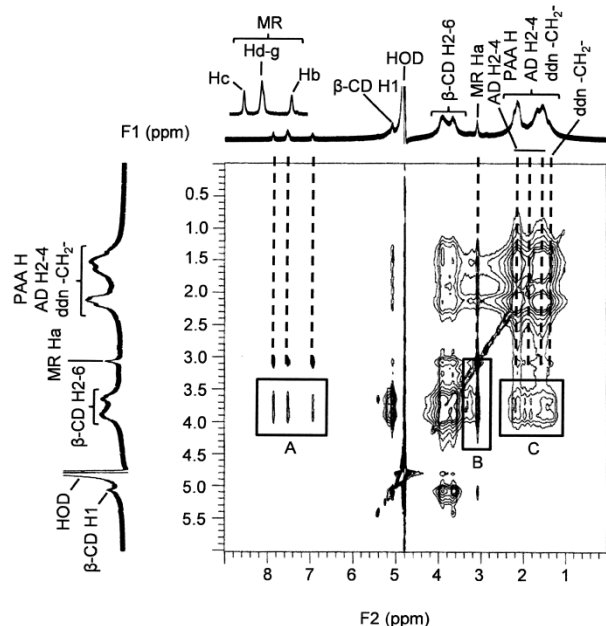


Figure S36: 2D NOESY ^1H NMR spectrum of MR ($[\text{MR}] = 2.0 \times 10^{-3} \text{ mol dm}^{-3}$) and PAA β -CDen (0.78 wt %, $[\beta\text{-CDen}] = 3.6 \times 10^{-3} \text{ mol dm}^{-3}$) and PAAADddn (0.42 wt %, $[\text{ADddn}] = 1.2 \times 10^{-3} \text{ mol dm}^{-3}$) in D_2O $\text{Na}_2\text{HPO}_4/\text{KH}_2\text{PO}_4$ buffer solution at $\text{pD} = 7.0$ and $I = 0.10 \text{ mol dm}^{-3}$ at 298.2 K. Cross-peaks in boxes A and B arise from dipolar interactions between the annular H3,5,6 protons of β -CDen and the aromatic (Hb-g) and methyl (Ha) protons of MR, respectively. Cross-peaks in box C arise from dipolar interactions between the annular H3,5,6 protons of β -CDen and the H2-4 protons of ADddn and the tether dodecyl methylene protons.

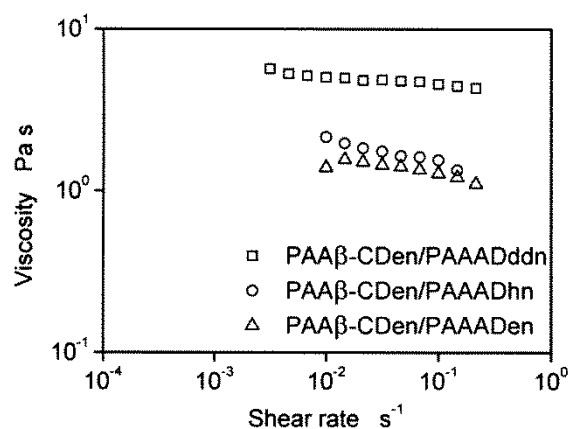


Figure S37: Viscosity variations with shear rate at 298.2 K of aqueous $\text{Na}_2\text{HPO}_4/\text{KH}_2\text{PO}_4$ buffered solutions ($\text{pH} 7.0$ and $I = 0.10 \text{ mol dm}^{-3}$) of (g) 1.20 wt % PAA β -CDen/PAAAddn: (0.78 wt %, $[\beta\text{-CDen}] = 3.60 \times 10^{-3} \text{ mol dm}^{-3}$) and PAAAddn (0.42 wt %, $[\text{ADddn}] = 1.20 \times 10^{-3} \text{ mol dm}^{-3}$), (h) 1.18 wt % PAA β -CDen/PAAADhn: (0.78 wt %, $[\beta\text{-CDen}] = 3.60 \times 10^{-3} \text{ mol dm}^{-3}$) and PAAADhn (0.40 wt %, $[\text{ADhn}] = 1.20 \times 10^{-3} \text{ mol dm}^{-3}$) and (i) 1.14 wt % PAA β -CDen/PAAADen: PAA β -CDen (0.78 wt %, $[\beta\text{-CDen}] = 3.60 \times 10^{-3} \text{ mol dm}^{-3}$) and PAAADen (0.36 wt %, $[\text{ADen}] = 1.20 \times 10^{-3} \text{ mol dm}^{-3}$). These solutions correspond to (g), (h) and (i) in Table S1, but contain no dye.

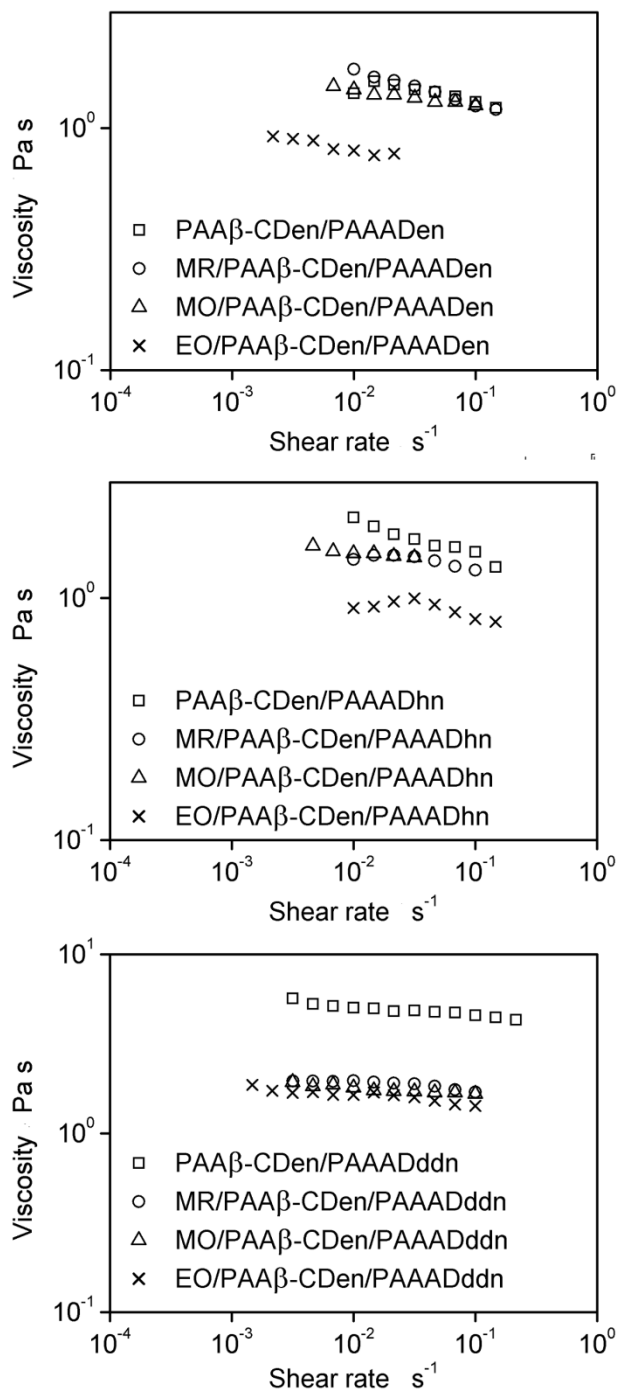


Figure S38: Viscosity variations with shear rate at 298.2 K of aqueous $\text{Na}_2\text{HPO}_4/\text{KH}_2\text{PO}_4$ buffered solutions (pH 7.0 and $I = 0.10 \text{ mol dm}^{-3}$) of (Top) (i) 1.14 wt % PAA β -CDen/PAAADen: PAA β -CDen (0.78 wt %, $[\beta\text{-CDen}] = 3.60 \times 10^{-3} \text{ mol dm}^{-3}$) and PAAADen (0.36 wt %, $[\text{ADen}] = 1.20 \times 10^{-3} \text{ mol dm}^{-3}$), (Middle) (h) 1.18 wt % PAA β -CDen/PAAADhn: (0.78 wt %, $[\beta\text{-CDen}] = 3.60 \times 10^{-3} \text{ mol dm}^{-3}$) and PAAADhn (0.40 wt %, $[\text{ADhn}] = 1.20 \times 10^{-3} \text{ mol dm}^{-3}$) and (Bottom) (g) 1.20 wt % PAA β -CDen/PAAADddn: (0.78 wt %, $[\beta\text{-CDen}] = 3.60 \times 10^{-3} \text{ mol dm}^{-3}$) and PAAADddn (0.42 wt %, $[\text{ADddn}] = 1.20 \times 10^{-3} \text{ mol dm}^{-3}$) and $2.00 \times 10^{-3} \text{ mol dm}^{-3}$ MR, MO or EO. These solutions correspond to (i), (h) and (g) in Table S1.

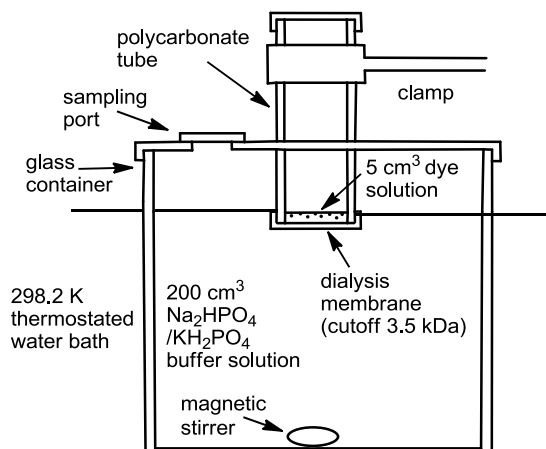


Figure S39: Schematic illustration of dye release measurement apparatus.

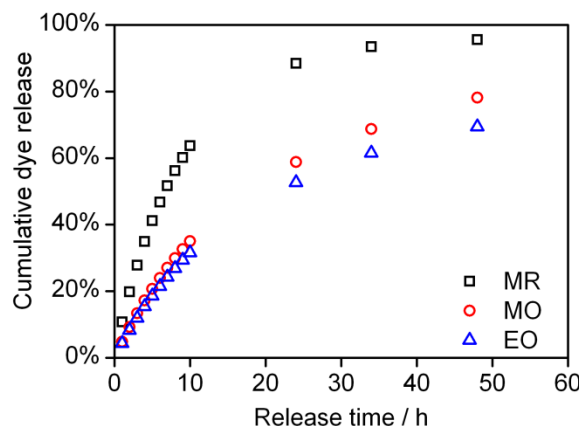


Figure S40: Release profiles of three dyes from a (j) 1.18 wt % PAA/PAA β -CDen aqueous $\text{Na}_2\text{HPO}_4/\text{KH}_2\text{PO}_4$ buffer solution at pH 7.0 and $I = 0.10 \text{ mol dm}^{-3}$ at 298.2 K. The dye concentration = $2.00 \times 10^{-3} \text{ mol dm}^{-3}$.

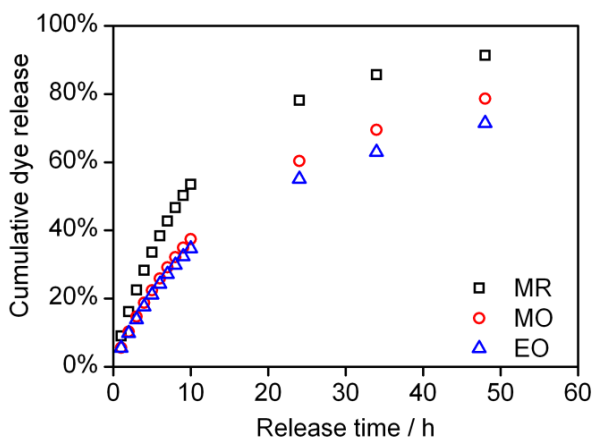


Figure S41: Release profiles of three dyes from a (i) 1.14 wt % PAA β -CDen/PAAADen/dye $\text{Na}_2\text{HPO}_4/\text{KH}_2\text{PO}_4$ aqueous buffer solution at pH 7.0 and $I = 0.10 \text{ mol dm}^{-3}$ at 298.2 K. The initial dye concentration = $2.00 \times 10^{-3} \text{ mol dm}^{-3}$.

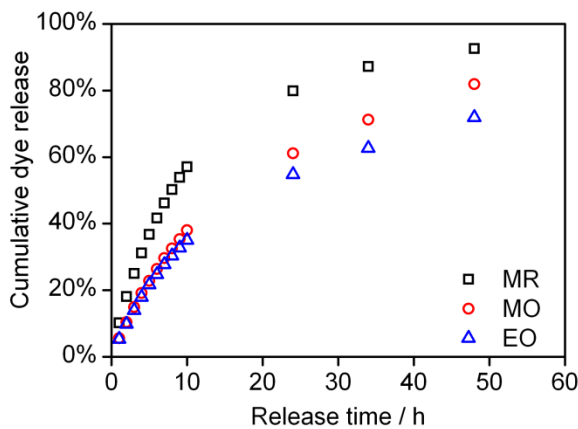


Figure S42: Release profiles of three dyes from a (h) 1.18 wt % PAA β -CDen/PAAADhn aqueous $\text{Na}_2\text{HPO}_4/\text{KH}_2\text{PO}_4$ buffer solution at pH 7.0 and $I = 0.10 \text{ mol dm}^{-3}$ at 298.2 K. The dye concentration = $2.00 \times 10^{-3} \text{ mol dm}^{-3}$.

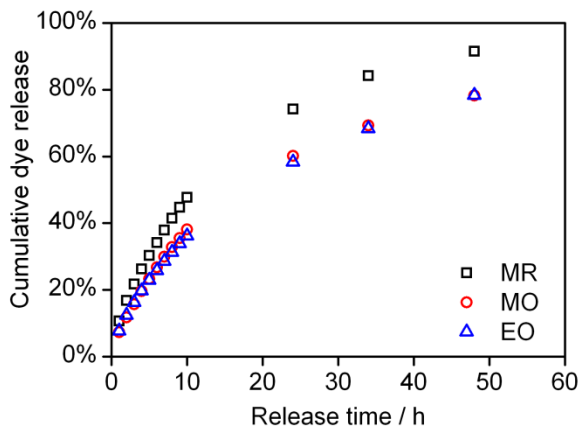


Figure S43: Release profiles of three dyes from a (g) 1.20 wt % PAA β -CDen/PAAADddn aqueous $\text{Na}_2\text{HPO}_4/\text{KH}_2\text{PO}_4$ buffer solution at pH 7.0 and $I = 0.10 \text{ mol dm}^{-3}$ at 298.2 K. The dye concentration = $2.00 \times 10^{-3} \text{ mol dm}^{-3}$.

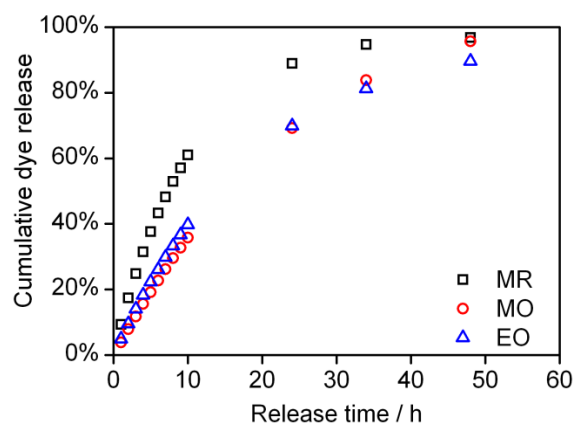


Figure S44: Release profiles of three dyes from a (f) 1.20 wt % PAA/β-CD aqueous $\text{Na}_2\text{HPO}_4/\text{KH}_2\text{PO}_4$ buffer solution at pH 7.0 and $I = 0.10 \text{ mol dm}^{-3}$ at 298.2 K. The dye concentration = $2.00 \times 10^{-3} \text{ mol dm}^{-3}$.

Table S1: Composition of solutions for dye release studies.^{1,2}

Solution	Composition
(a) Na ₂ HPO ₄ /KH ₂ PO ₄ buffer	pH = 7.0, $I = 0.10 \text{ mol dm}^{-3}$
(b) 1.20 wt % PAA	PAA, 1.20 wt %
(e) 1.14 wt % PAA/PAAADen	PAAADen, 0.36 wt %, [ADen substituents] = $1.20 \times 10^{-3} \text{ mol dm}^{-3}$ PAA, 0.78 wt %, total wt % = 1.14
(d) 1.18 wt % PAA/PAAADhn	PAAADhn, 0.40 wt %, [ADhn substituents] = $1.20 \times 10^{-3} \text{ mol dm}^{-3}$ PAA, 0.78 wt %, total wt % = 1.18
(c) 1.20 wt % PAA/PAAADddn	PAAADddn, 0.42 wt %, [ADddn substituents] = $1.20 \times 10^{-3} \text{ mol dm}^{-3}$ PAA, 0.78 wt %, total wt % = 1.20
(f) 1.20 wt % PAA/β-CD	$[\beta\text{-CD}] = 3.60 \times 10^{-3} \text{ mol dm}^{-3}$ PAA, 1.20 wt %, total wt % = 1.20
(j) 1.18 wt % PAA/β-CDen	PAAβ-CDen, 0.78 wt %, [β-CDen substituents] = $3.60 \times 10^{-3} \text{ mol dm}^{-3}$ PAA, 0.40 wt %, total wt % = 1.18
(i) 1.14 wt % PAAβ-CDen/PAAADen	PAAβ-CDen, 0.78 wt %, [β-CDen substituents] = $3.60 \times 10^{-3} \text{ mol dm}^{-3}$ PAAADen, 0.36 wt %, total wt % = 1.14 [ADen substituents] = $1.20 \times 10^{-3} \text{ mol dm}^{-3}$
(h) 1.18 wt % PAAβ-CDen/PAAADhn	PAAβ-CDen, 0.78 wt %, [β-CDen substituents] = $3.60 \times 10^{-3} \text{ mol dm}^{-3}$ PAAADhn, 0.40 wt %, total wt % = 1.18 [ADhn substituents] = $1.20 \times 10^{-3} \text{ mol dm}^{-3}$
(g) 1.20 wt % PAAβ-CDen/PAAADddn	PAAβ-CDen, 0.78 wt %, [β-CDen substituents] = $3.60 \times 10^{-3} \text{ mol dm}^{-3}$ PAAADddn, 0.42 wt %, total wt % = 1.20 [ADddn substituents] = $1.20 \times 10^{-3} \text{ mol dm}^{-3}$
(l) 1.89 wt % PAAβ-CDen/PAAADen	PAAβ-CDen, 1.30 wt %, [β-CDen substituents] = $6.00 \times 10^{-3} \text{ mol dm}^{-3}$ PAAADen, 0.59 wt %, total wt % = 1.89 [ADen substituents] = $2.00 \times 10^{-3} \text{ mol dm}^{-3}$
(k) 1.96 wt % PAAβ-CDen/PAAADhn	PAAβ-CDen, 1.30 wt %, [β-CDen substituents] = $6.00 \times 10^{-3} \text{ mol dm}^{-3}$ PAAADhn, 0.66 wt %, total wt % = 1.96 [ADhn substituents] = $2.00 \times 10^{-3} \text{ mol dm}^{-3}$

¹Solutions are labelled in the same order as in Figure 12 in the main manuscript.²All solutions were prepared in aqueous Na₂HPO₄/KH₂PO₄ buffer at pH 7.0 and $I = 0.10 \text{ mol dm}^{-3}$ at 298.2 K. Dye concentration was $2.00 \times 10^{-3} \text{ mol dm}^{-3}$ for all samples.